Effect of Poly(ethylene glycol) on the Properties and Foaming Behavior of Macroporous Poly(lactic acid)/Sodium Chloride Scaffold

Bin-Yi Chen, Yuan-Sheng Wang, Hao-Yang Mi, Peng Yu, Tai-Rong Kuang, Xiang-Fang Peng, Jing-Song Wen

School of Mechanical and Automotive Engineering, National Engineering Research Center of Novel Equipment for Polymer Processing, Key Laboratory of Polymer Processing Engineering of Ministry of Education, South China University of Technology, Guangzhou 510640, China
Correspondence to: X.-F. Peng (E-mail: pmxfpeng@scut.edu.cn) and J.-S. Wen (E-mail: jswen@scut.edu.cn)

ABSTRACT: In this study, we prepared poly(lactic acid) (PLA)/poly(ethylene glycol) (PEG)/sodium chloride (NaCl) blends by melt blending with a triple-screw dynamic extruder. The effects of PEG on the thermal property, mechanical property, and morphology of blends were investigated in detail. It was found that the incorporation of PEG and NaCl significantly improved the crystallization rate, elongation at break, surface adhesion, and reduced viscoelasticity of PLA. The blends were further batch-foamed at different temperatures with supercritical carbon dioxide to study the foaming properties. The results of PLA/PEG/NaCl (50 : 10 : 40 wt %) composites after foaming and particle leaching revealed that an interconnected bimodal porous scaffold with the highest porosity of 89% could be achieved. Furthermore, the addition of PEG can significantly reduce the water contact angle so as to enhance the wetting ability of the scaffolds. © 2014 Wiley Periodicals, Inc. J. Appl. Polym. Sci. **2014**, *131*, 41181.

INTRODUCTION

Tissue engineering is an interdisciplinary subject composed of materials science, life science, and engineering that has been extensively researched to create biological alternatives for implants and prostheses over the past few decades. An ideal scaffold should have a specific three-dimensional (3D) shape, appropriate pore size, high porosity, and pore interconnectivity.[1–3] It is reported that the scaffold with multiple size of pores is critical in seeding and adhesion of cells and growing of new tissue.[4] Various pore sizes are designed for different functions, like large pores for cell growth and proliferation and small pores for the diffusion of nutrients and/or metabolites.[5] Thus, the development of new methods for creating such structured materials is a central concern.

Currently available techniques for fabricating polymer porous scaffold such as solvent casting,[6] particle leaching,[7,8] electrostatic spinning,[9] freeze drying,[10] solid freeform fabrication,[11] gas foaming,[12,13] and phase separation[14] have been widely used. Among these methods, particle leaching is one of the most common techniques to fabricate scaffolds, which has been confirmed to be effective in controlling the porosity and pore size.[15] In the past few years, the combination of particle leaching with other

techniques has been widely investigated for tissue engineering applications. For example, Gong et al.[16] fabricated graded macroporous poly(lactic acid) (PLA) scaffold by a progressive solvent-casting/particle leaching approach, which obtained the grade pore size (from 166 ± 41 μm to 453 ± 18 μm) by gradually decreasing the size and content of salt at different layers. Aydin et al.[17] introduced naphthalene as the secondary porogen in the solvent-evaporation/particulate-leaching process to enhance pore interconnectivity of tissue engineering scaffolds. Kim et al.[18] produced macroporous and nanofibrous scaffolds with bioactive nanocomposite composition by using the phase separation process and salt particle leaching process to obtain porosities of 90–95% and pore sizes of over hundreds of micrometers. Most of the above-mentioned techniques are potentially toxic organic solvents involved, which can be detrimental to cell survival and tissue growth. The combination of melt-extrusion blending and gas foaming to prepare porous structures is proposed as an alternative method to avoid the organic solvents. However, PLA/sodium chloride (NaCl) composites were usually fabricated by hot compression in most of the studies.[12,19,20] Because of its high content, NaCl component was difficult to process by the traditional extruders; however, there are few studies about melt-extrusion PLA blends with NaCl.[21,22]

Table I. Compositions of the Blends

Samples	PLA (wt %)	PEG (wt %)	NaCl (wt %)
Neat PLA	100	–	–
A	70	–	30
B	60	–	40
C	60	10	30
D	50	10	40

An important class of biodegradable polymers includes aliphatic polyesters like PLA, poly(ξ-caprolactone) (PCL), polyglycolide (PGA), or their copolymers, which are approved by the Food and Drug Administration for certain clinical applications have been processed into scaffolds for tissue engineering.[23] As the representative of this family, PLA has been widely used in food packing, drug delivery, and tissue engineering fields.[24–26] However, its brittleness, degradation rate, and strong hydrophobicity have limited its applications. To overcome these problems, a large number of researches have been devoted to improve PLA properties by blending poly(ethylene glycol) (PEG) plasticizer.[27,28] Sheth et al.[29] prepared PLA/PEG blends at various PEG contents; it was found that the blends exhibited higher elongations and lower modulus values below 50% PEG content, and the enzymatic degradation shows that the weight loss for all of the blends was significantly greater than that for the pure PLA. Jiang and Liao[30] prepared PLA-b-PEG fibrous scaffolds by electrospinning, which exhibited good flexibility and an enhanced hydrophilicity. Wang et al.[31] fabricated the biodegradable PLA/PEG hybrid membranes via electrospinning. The results showed that the electrospinning process gradually became easy with increased PEG content, and the average diameter of fibers was at range of 1.79–3.01 μm. Moreover, there are also some works have been reported in the literature using a combination of inorganic (NaCl) and organic (PEG) porogens
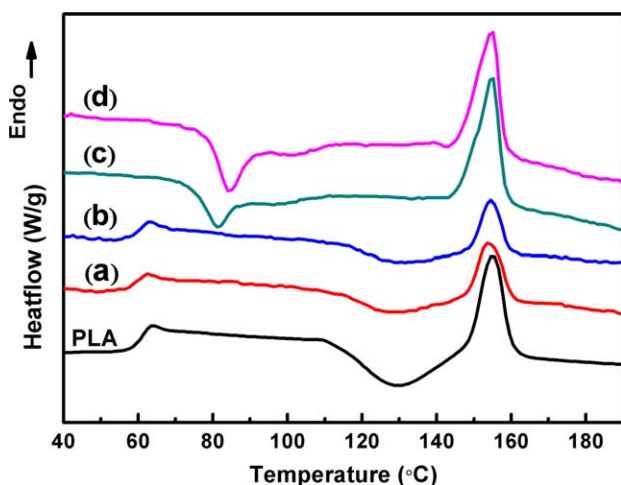
in particulate leaching method. For example, Liu et al.[32] fabricated tissue engineering scaffolds by combining NaCl and PEG as coporogens. Shokrolahi et al.[33] studied the polyurethane scaffolds for bone tissue engineering by compression molding and particle leaching method, a highly porous 3D scaffold (>85 vol %) with a well-interconnected porous structure achieved by this combinatory process. However, there are a few studies on the foaming behavior of PLA/PEG blends. Recently, we have developed a simple and versatile method for preparation of PLA/PEG scaffolds by melt extrusion and supercritical gas foaming, which obtained an interconnected structure with a maximum porosity of 82.3% with the incorporation of PEG; however, the pore size lacked a particular multiscaled porous structure.[34] The aim of this work was scheduled on a technique for fabricating bimodal porous scaffold with high porosity and open-pore structure from PLA/PEG/NaCl blends. To the best of our knowledge, no work has been reported in the literature using a combination of PEG and NaCl porogens in melt extrusion, gas foaming, and particulate leaching method. However, a large number of articles already reported for porous structure fabrication by the gas foaming and particulate leaching method.

In the study, the blends were melt-mixed with a home-made triple-screw dynamic extruder to prepare blend with optimized properties. Then, the blends were foamed to investigate the feasibility of bimodal and open-pore foam fabrication. The PEG was used as polymeric porogen, which was anticipated to improve the rupture of the pores during expansion and to create interconnected channels foamed pores. Moreover, the incorporation of amphiphilic PEG is anticipated to improve the hydrophilicity of PLA, which will be in favor of cell attachment and proliferation. The NaCl particles were used as porogen of macropores, which distributed in the foams to create bimodal porosity. To study the effect of PEG on the viscoelastic properties of the composites, which is directly related to the open-pore structure during decompression, it is important to learn about the foaming parameters, in particular foaming temperature. Because the incorporation of PEG radically reduced the elasticity and viscosity with the increase of foaming temperature, which will make the matrix melt too weak to sustain the pore growth and expansion. The optimized blends were further batch-foamed at different temperatures with supercritical carbon dioxide (CO_2) to investigate the foaming behavior. The thermal properties, mechanical properties, rheological behavior, and morphology of the blends, as well as the pore morphology, residual content of porogen, and the hydrophilicity of the foams, were discussed in detail.
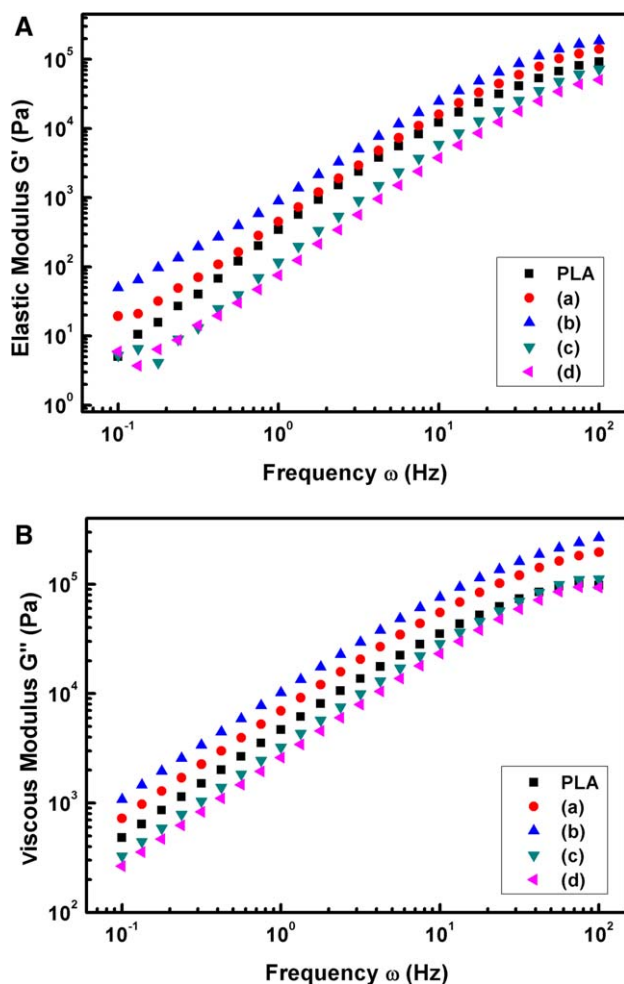

Figure 1. DSC thermograms of PLA and PLA composites: (a) PLA/NaCl (70 : 30 wt %), (b) PLA/NaCl (60 : 40 wt %), (c) PLA/PEG/NaCl (60 : 10: 30 wt %), and (d) PLA/PEG/NaCl (50 : 10 : 40 wt %). [Color figure can be viewed in the online issue, which is available at wileyonlinelibrary.com.]

Table II. Thermal Properties of PLA and PLA Composites

Samples	T_g (°C)	T_{cc} (°C)	T_m (°C)
Neat PLA	61.3	129.6	155.0
A	60.1	127.9	154.2
B	60.9	128.2	154.4
C	–	81.5	154.8
D	–	84.4	154.8

Figure 2. (A) Storage modulus (G') and (B) loss modulus (G'') as a function of frequency for PLA and PLA composites at temperature of 170°C: (a) PLA/NaCl (70 : 30 wt %), (b) PLA/NaCl (60 : 40 wt %), (c) PLA/PEG/NaCl (60 : 10 : 30 wt %), and (d) PLA/PEG/NaCl (50 : 10 : 40 wt %). [Color figure can be viewed in the online issue, which is available at wileyonlinelibrary.com.]

EXPERIMENTAL

Materials

PLA (2002D, $M_w = 250{,}000$ g/mol) with D-lactide content of 4% was purchased from Natureworks, and it had a density of 1.29 g/cm^3. PEG with a molecular weight of 6000 g/mol was supplied by Aoki Grease Industry Corporation. NaCl as the water-soluble porogen was grinded and sieved to 40–75 μm. All materials were used as received.

Processing of Blends

PLA and NaCl particles were predried in a vacuum oven at 80°C for 8 h, and PEG was dried at 40°C for 4 h. The PEG was blended with NaCl particles and PLA via a self-designed triple-screw dynamic extruder to improve the mixability and dispersion of NaCl particles.[35–37] Melt-blending processing was performed at a constant rotor speed of 60 rpm, and the temperature profile from hopper to the die was set from 130 to 170°C. The experiment formulae are listed in Table I. The mixtures were extruded using a four-strand die followed by ambient

cooling and pelletizing. The pellets were compression molded to plates with the thickness of 1 and 4 mm at 190°C.

Foaming Process

The foaming behavior was investigated using CO_2 as the physical foaming agent via a customized batch foaming device, which is connected to a supercritical fluid pumping unit. The samples used for batch foaming were cut from the compress-molded plates. The CO_2 pressure and temperature were controlled by the supercritical fluid pump and the thermocouple, respectively. The autoclave was heated to 160°C and pressurized with CO_2 at 20 MPa for 1 h to ensure sorption equilibrium of the entire sample. After CO_2 sorption, the temperature was reduced to 90, 100, and 110°C, respectively. Then, the CO_2 pressure was instantaneously depressurized to atmospheric pressure to induce bubble nucleation and growth. The solidification of the porous structure was achieved by a water-cooling system.

Particle Leaching Process

To dissolve the salt particles, the foamed and unfoamed samples were immersed in a water bath at 45°C, and the water was changed every 12 h until the sample obtained constant weight. After leaching, the samples were dried and stored in a drying vessel until further use.
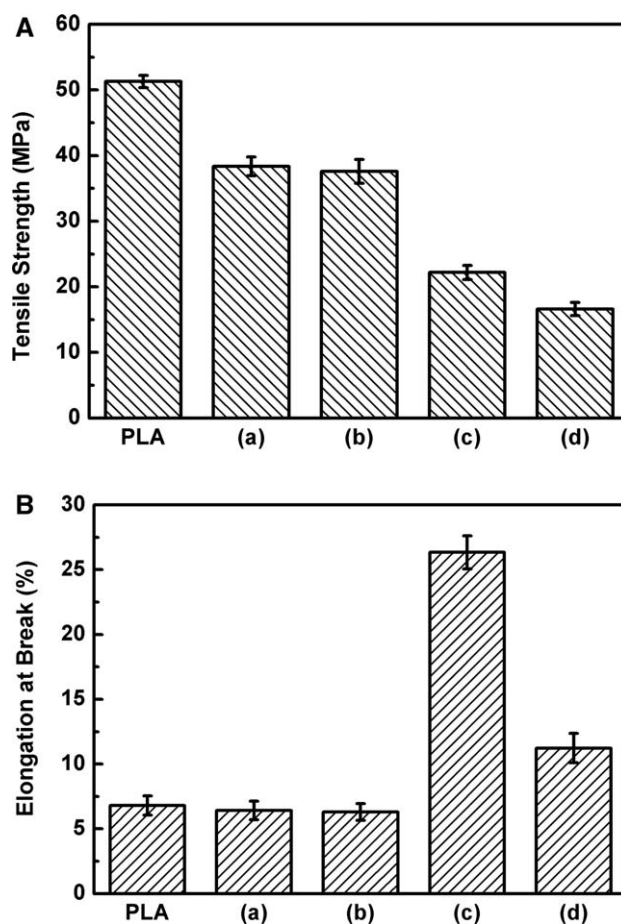
Figure 3. (A) Tensile strength and (B) elongation at break of PLA and PLA composites: (a) PLA/NaCl (70 : 30 wt %), (b) PLA/NaCl (60 : 40 wt %), (c) PLA/PEG/NaCl (60 : 10 : 30 wt %), and (d) PLA/PEG/NaCl (50 : 10: 40 wt %).
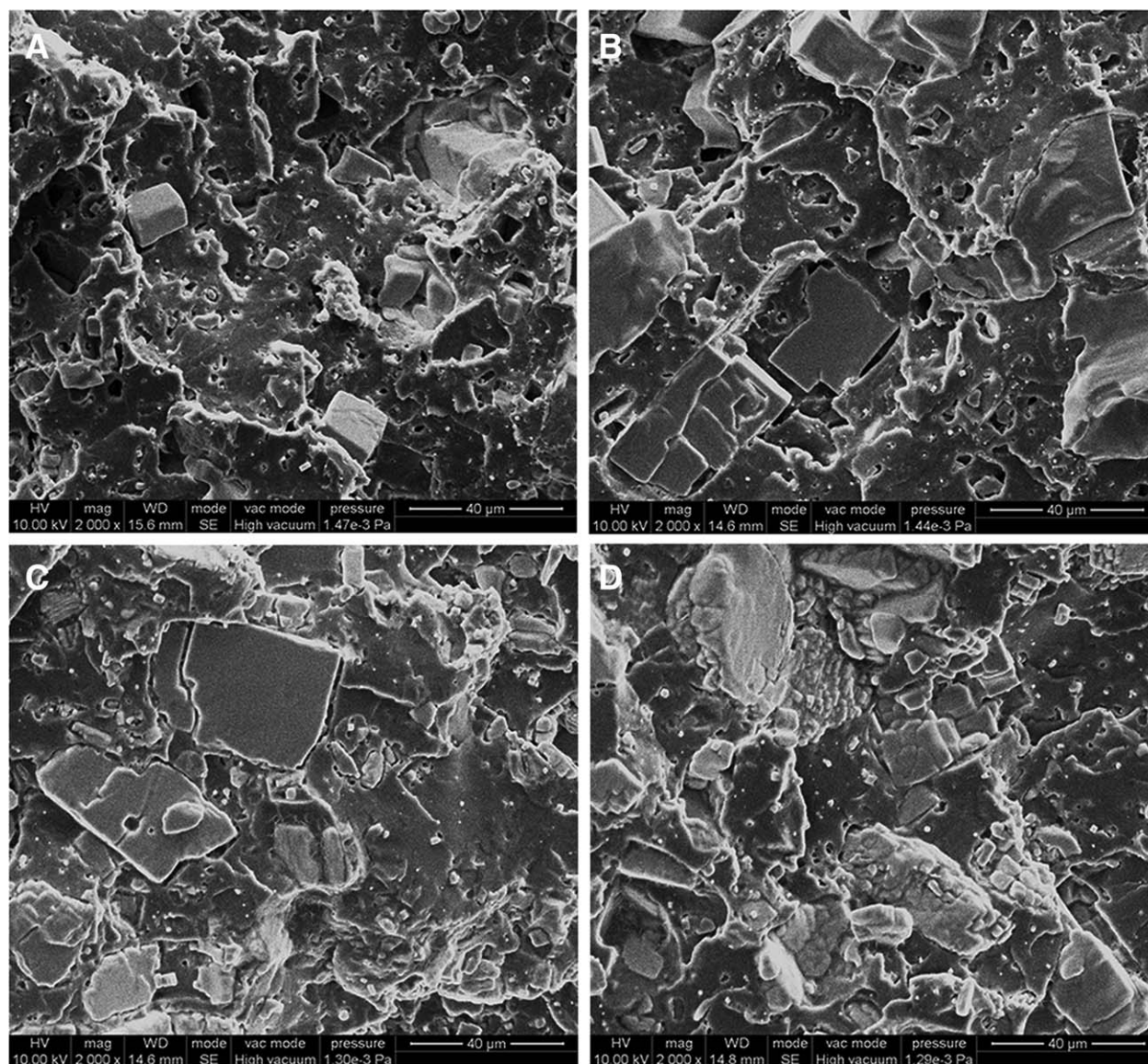
Figure 4. SEM micrographs of solid PLA matrix: (A) PLA/NaCl (70 : 30 wt %), (B) PLA/NaCl (60 : 40 wt %), (C) PLA/PEG/NaCl (60 : 10 : 30 wt %), and (D) PLA/PEG/NaCl (50 : 10 : 40 wt %).

Characterization

Differential Scanning Calorimetry. Differential scanning calorimetry (DSC) was carried out under nitrogen flow at a heating and cooling rate of 10°C/min to investigate the thermal properties of neat PLA and blends with DSC 204C (Netzsch, Germany). The specimens were sliced from the extruded pellets and then crimp-sealed in aluminum crucibles. All samples were first heated to 200°C and kept at isothermal condition for 5 min to release previous thermal history. Then, the samples were cooled to 30°C and subsequently scanned between 30 and 200°C.

Rheological Measurement. The influence of PEG and NaCl particles on the rheological properties of the matrix was investigated by a Bohlin Gemini 200 Rheometer equipped with a parallel-plate fixture (25 mm diameter). Dynamic complex viscosity (η^*) and the storage moduli (G') as functions of angular frequency (ω) ranging from 0.1 to 100 rad/s were measured at

170°C. The measurements were carried out at a nitrogen atmosphere. Samples for the rheological test were machined from the 1-mm-thick compress-molded plates.

Mechanical Properties. The tensile testing of neat PLA and PLA blends was carried out by a universal test system (Instron 5566). The crosshead speed was 1 mm/min, and at least five samples for each formulation were selected to guarantee the accuracy.

Scanning Electron Microscopy. The NaCl particles dispersion in the PLA matrix and the pore morphology of the samples before and after leaching were observed via the S-3700N (Hitachi, Japan) scanning electron microscopy operated at 10 KV. Samples were immersed in liquid nitrogen for 30 min to maintain the pore structure before cryogenic fracture, and then, all samples were sputter-coated with a thin layer of gold (-20 nm)
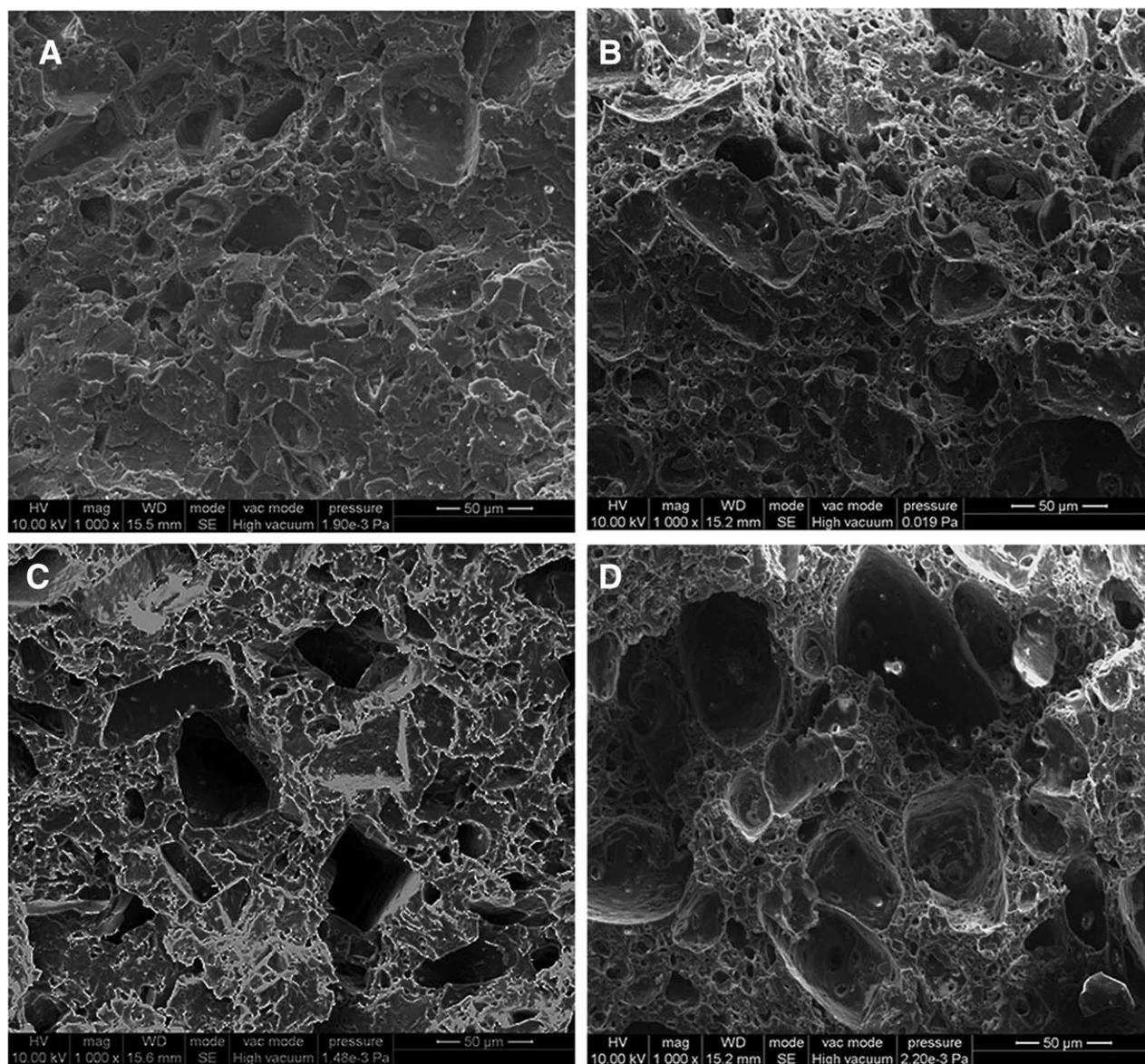
Figure 5. SEM micrographs of solid PLA matrix after leaching: (A) PLA/NaCl (70 : 30 wt %), (B) PLA/NaCl (60 : 40 wt %), (C) PLA/PEG/NaCl (60 : 10 : 30 wt %), and (D) PLA/PEG/NaCl (50 : 10 : 40 wt %).

prior to examination. The pore size was calculated using the Image-Pro Plus software, and the apparent density (ρ_{app}) of the foam samples was measured by pycnometer method. The porosity of the foam samples was determined by the following equation[38]:

$$V_f = \left(1 - \frac{\rho_{app}}{\rho_{PLA}}\right) \times 100\%, \qquad (1)$$

where V_f is the porosity of the sample, and ρ_{PLA} is the density of the neat PLA, which is 1.31 g/cm^3.

Thermogravimetric Analysis. The residual PEG and NaCl particles after leaching were determined by a Perkin Elmer thermogravimetric analyzer. All samples were heated from room temperature to 600°C at a ramp speed of 40°C/min. The early

decomposition is contributed by PEG, and the residual weight is contributed by NaCl.

Contact Angle Measurement. To investigate the effect of PEG on the hydrophilicity of the scaffolds, PLA scaffolds were examined by water contact angle measurements (OCA 400 Micro, Dataphysics, Germany) at room temperature. The pure PLA, PLA/NaCl, and PLA/PEG/NaCl foams after leaching were measured. Because of rapid cooling during foaming processing, the sample formed a thin layer of solid skin. There was no pore in this solid skin after leaching. To avoid the interference of the pores on the data, a drop of distilled water was dropped on the solid skin of the leached specimens and photographed immediately by a digital camera. The contact angles were measured on digital photographs using image analysis software. At least five measurements were performed for each sample.
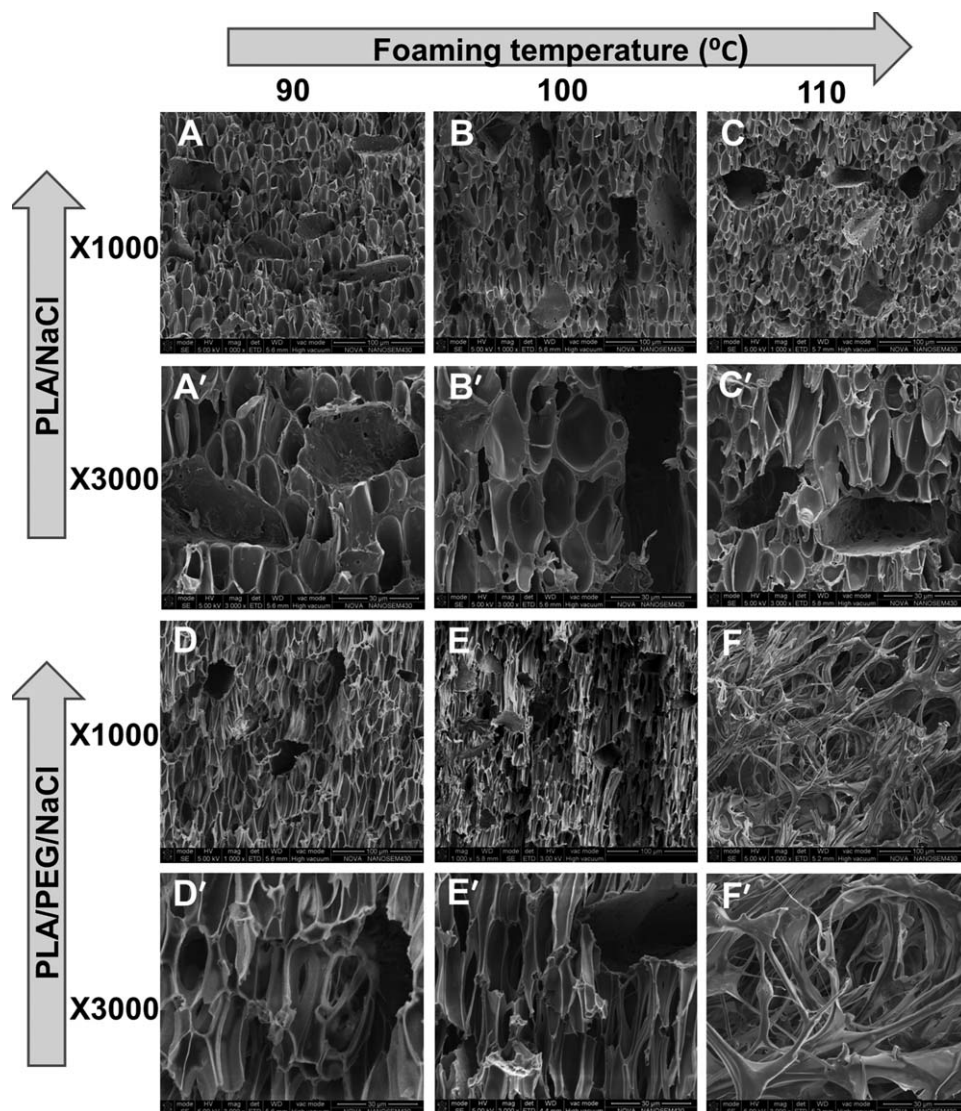
Figure 6. Foam morphology of PLA/NaCl (A–C and A′–C′) and PLA/PEG/NaCl (D–F and D′–F′) after leaching as a function of foaming temperatures (A, A′, D, D′ are at 90°C, B, B′, E, E′ are at 100°C, and C, C′, F, F′ are at 110°C) at ×1000 magnification (A–C and D–F) and ×3000 magnification (A′–C′ and D′–F′). [Correction added on 24 July 2014, after first online publication: Graphic was replaced due to typographical error and degree symbol added to temperature units in legend]

RESULTS AND DISCUSSION

Thermal Properties

The DSC scans of all the melt-extruded specimens are shown in Figure 1, and the characteristic temperatures are listed in Table II. The glass transition temperature (T_g) was taken as the midpoint of the inflection, and the melting points were the peak temperatures of the melting endotherms. The pure PLA shows a distinct glass transition with T_g at ∼61°C. When compared with pure PLA, the T_g of PLA/NaCl blends decreases slightly. However, for PLA/PEG/NaCl blends, the T_g could not be observed by DSC, which was due to enhanced segmental mobility of PLA chains caused by the presence of plasticizer PEG.

Above glass transition, all samples exhibit an exothermic broad peak of cold crystallization. The curves show that the cold crystallization temperature (T_{cc}) of PLA/NaCl blends is almost the same as that of PLA. When 10% PEG was present, the cold

crystallization exotherms still exist, whereas the T_{cc} shifts to lower temperature (i.e., 85°C) conceivably because of the increased crystallization rate of PLA with additional PEG. Similar results of T_{cc} decrease in parallel with the shift in T_g were also proved by the results of Wang et al.,[31] which suggested that the PEG increased the crystallization rate of PLA. The curves and the data in Table II show that the T_g, T_{cc}, and T_m slightly decrease with the increasing NaCl content. The significant change in crystallization behavior of PLA/PEG/NaCl hybrid is due to the increase of chain motion attributed to the addition of PEG, which induced an easier rearrangement of polymer chains to crystallize.

Rheological Properties

The additions of plasticizer and microsized fillers to a polymer melt have complex influences on the rheological properties of
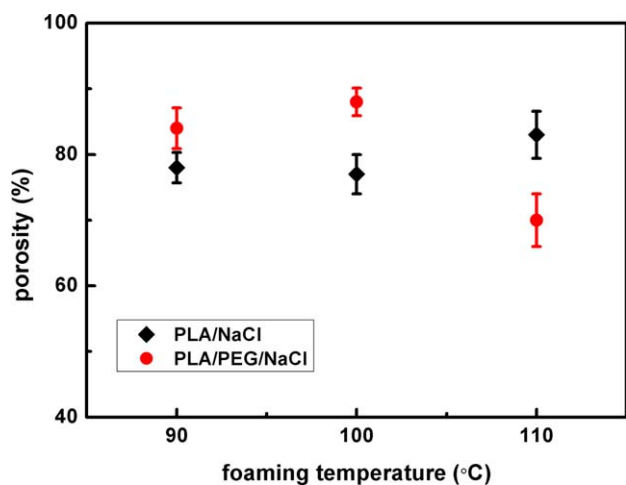
Figure 7. Porosity of PLA/NaCl and PLA/PEG/NaCl microcellular foamed at different foaming temperatures. [Color figure can be viewed in the online issue, which is available at wileyonlinelibrary.com.]

the composite. In this study, the influence of PEG and NaCl on the rheological properties of the matrix was investigated by dynamic oscillatory shear measurement. The storage modulus (G') and loss modulus (G'') as a function of frequency are shown in Figure 2. The curves show that the neat and filled PLA melts exhibit viscoelastic behaviors, which are a combination of reversible elastic deformations due to molecular chain entanglements and irreversible viscous flows due to polymer chain slippage. It is noticed that the G' and G'' of PLA/NaCl blends are higher than that of neat PLA. The increase in the modulus is attributed to a filler network formed in the blends. However, the addition of PEG to PLA/NaCl blends makes the storage and loss moduli lower than those of PLA/NaCl, which is due to the fact that micromolecule plasticizer increased the chain mobility and polymer-free volume to reduce the shear viscosity of the blends. This result agrees with our previously reported rheological results of PLA/PEG matrix by capillary rhe-
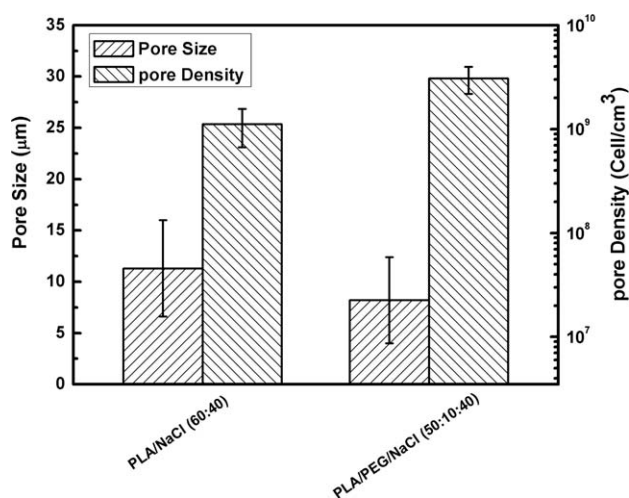
Figure 8. Average cell size and cell density of microcellular PLA/NaCl and PLA/PEG/NaCl blends obtained from SEM analysis.

ometer.[34] It is well known that the pore nucleation and the following pore expansion during foaming are closely associated with the viscoelasticity of the matrix, which will significantly affect the foam morphology. As shown in Figure 2, the PLA/PEG/NaCl matrix with 40 wt % NaCl showed the lowest viscoelasticity. This lowest viscoelasticity could more easily result in the pores break at the pore wall during pore expansion to increase the open-pore quantities, which will be discussed in the following section.

Mechanical Properties

The mechanical properties of neat PLA and blends were studied by tensile testing. The tensile strength and the elongation at break curves are shown in Figure 3. As expected, the addition of PEG significantly changes the tensile behavior of the PLA. Neat PLA is very rigid and brittle. The tensile strength is 54.9 MPa, whereas the elongation at break is only about 6.86%. After incorporating NaCl into PLA, the average tensile strength decreased obviously. It shows that the average tensile strength of the matrices decreased with various NaCl concentrations. For the PLA/PEG/NaCl blends, the average tensile strength further reduces. The lowest tensile strength of PLA/PEG/NaCl with 40 wt % NaCl is only 16.62 MPa. It is interesting to note that the average elongation at break significantly increases with the incorporation of PEG. When compared with neat PLA, the PLA/PEG/NaCl blends with different contents of NaCl (30 and 40 wt %), the tensile strength decreased from 54.9 MPa to 22.18 MPa and 16.62 MPa, whereas the average elongation at break increased from 6.86% to 26.34% and 11.27%. This result is consistent with the prior results from Sheth et al.[29] and Park et al.[39] The mechanical properties indicate that the addition of the PEG increases the flexibility of the blends system.

Phase Morphology of PLA Blends

The fractured surfaces of PLA/NaCl and PLA/PEG/NaCl blends were examined using SEM to evaluate the size, shape, and dispersion of NaCl in the PLA matrix. The fractured surfaces of the solid PLA/NaCl and PLA/PEG/NaCl blends are shown in Figure 4. As can be seen from Figure 4, the fractured surface without visible plastic deformation indicated a typical brittle fracture surface. The triple-screw dynamic extruder can generate high shear stress and extend melt-processing time in the barrel, which is positive to intensify the mixability and dispersion of NaCl particles in the PLA matrix. Moreover, the morphology exhibits the majority of the NaCl particles fractured to smaller size by the intensive shear of triple-screw melt extrusion. As shown in Figure 4(A,B), the NaCl particles and voids formed by NaCl particles, which are pulled out of the PLA matrix were seen, indicated that the interfacial affinity between PLA and NaCl is weak. In contrast, with the incorporation of PEG, the micrographs clearly show that the NaCl particles were embedded into the PLA matrix with large interpenetrating structure [Figure 4(C,D)]. Neither void formation around the NaCl particles nor cavities in the PLA matrix are observed. It is obvious to find that PLA/PEG/NaCl blend shows a better interfacial adhesion when compared with PLA/NaCl. The PEG plasticizer is positive to improved adhesion between PLA and NaCl mixed matrix, which would help to improve the dispersion of macropores in the foams after NaCl leaching.

The PLA blends with NaCl samples were leached with warm water, and the microstructures were examined by SEM. The morphological observations (Figure 5) showed that the pore morphology obtained primarily resembled the NaCl particles size and shape, with an average pore size of 50 μm. The porosity increases with the increase of NaCl content. However, NaCl particles were still entrapped in the sample of PLA/NaCl [Figure 5(A,B)] after leaching. Figure 5(C,D) clearly shows that the NaCl pores were deeply embedded into the PLA matrix. Furthermore, the incorporation of PEG increased the porosity as well as the extraction of the NaCl particles. It is worth noting that there are a large number of pores in the samples with 40 wt % NaCl. However, SEM images also showed lack of interconnectivity.

Foaming Properties of PLA/NaCl and PLA/PEG/NaCl Blends

According to previous discussion, the PLA/PEG/NaCl matrix with 40 wt % NaCl exhibited optimum properties, such as the lowest viscoelasticity (i.e., G' and G'') as well as the increased crystallization rate, which is positive for nucleation and open-pore formation during gas foaming. Moreover, the higher the content of NaCl, the higher quantities of large pores and porosity are obtained. In this section, porous scaffolds were thus prepared based on the matrices with 40 wt % NaCl by a customized batch-foaming device using supercritical CO_2 as the blowing agent. The foaming temperature was selected between 90 and 110°C to study the foaming properties of PLA/NaCl and PLA/PEG/NaCl blends.

To further enhance the porosity and bimodal porous structure of foamed blends, water leaching process was performed. Figure 6 shows the morphologies of the PLA/NaCl and PLA/PEG/NaCl foams after leaching at different foaming temperatures and magnifications. As evidenced by the SEM images, the NaCl particles disappeared after leaching, demonstrating that most of the salt particles were extracted. The residual content of NaCl was determined by thermogravimetric analysis in the following part. At a constant foaming temperature, the foam morphologies of the PLA/NaCl samples show bimodal porous structure, in which the large pores are caused by leaching out of NaCl particles and the small pores are foamed by CO_2. From the high magnification image, it is found that there is lack of interconnection channels between the pores. The foamed samples of PLA/PEG/NaCl after leaching also show double-scale porous structure; moreover, the high-magnification image shows an open-pore structure and higher pore interconnections when compared with the PLA/NaCl sample. This is because the PEG, which acted as a plasticizer, significantly reduced the elasticity and viscosity of the matrix, which may decrease the pore-wall strength, thus, the pores tend to break during foaming process, resulting in an open-pore structure. Furthermore, the leaching process would dissolve PEG as well as NaCl and cause interconnection channels.

The effect of the foaming temperature (90, 100 and 110°C, respectively) was also evaluated from Figure 6. For the PLA/NaCl foams, the foam morphologies slightly changed with the increasing foaming temperature. Only a few pores ruptured and coalesced at the higher foaming temperatures. For the PLA/
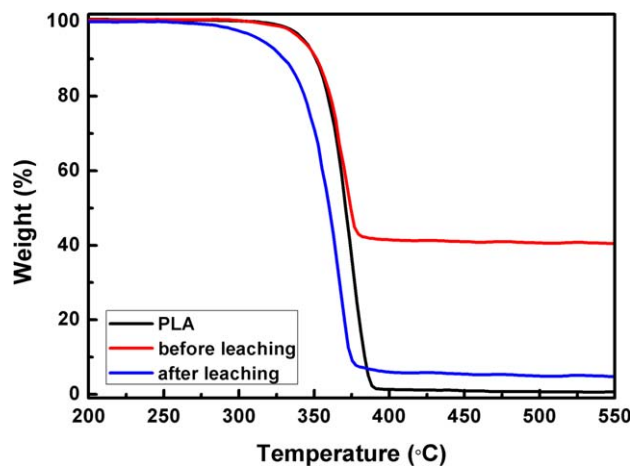
Figure 9. TGA curve of PLA and PLA/NaCl (60 : 40 wt %) samples before and after leaching. [Color figure can be viewed in the online issue, which is available at wileyonlinelibrary.com.]

PEG/NaCl foams, elevating the foaming temperature radically increased the pore coalescence, which obtained finer open-pore structure. In particular, the pores are almost completely collapsed at foaming temperature of 110°C. The reason is that the incorporation of PEG radically reduced the elasticity and viscosity of the matrix with the increase of temperature, which results in less resistance for the bubbles to grow and to coalesce, hence increasing the open-pore structure and coalescence at the higher foaming temperature. The porosities of these foams were calculated by using eq. (1), and these data are shown in Figure 7. It is clear that the sample of PLA/PEG/NaCl foamed at 100°C obtained the highest porosity (89%) and finest foam morphology. However, the sample foamed at 110°C exhibits the lowest porosity, which was due to the serious coalescence.

The average pore size and pore density of microcellular PLA/NaCl and PLA/PEG/NaCl blends (foamed at 100°C) were qualitatively analyzed by the Image-Pro Plus software, and the results are shown in Figure 8. For the PLA/NaCl and PLA/PEG/NaCl specimens, the average pore size was about 11 μm
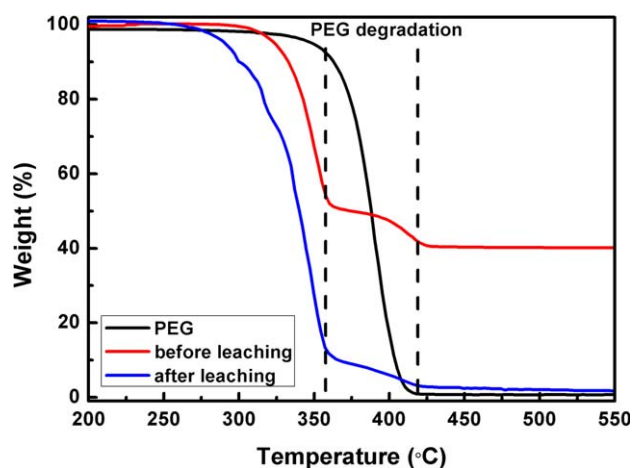
Figure 10. TGA curve of PEG and PLA/PEG/NaCl (50 : 10 : 40 wt %) samples before and after leaching. [Color figure can be viewed in the online issue, which is available at wileyonlinelibrary.com.]
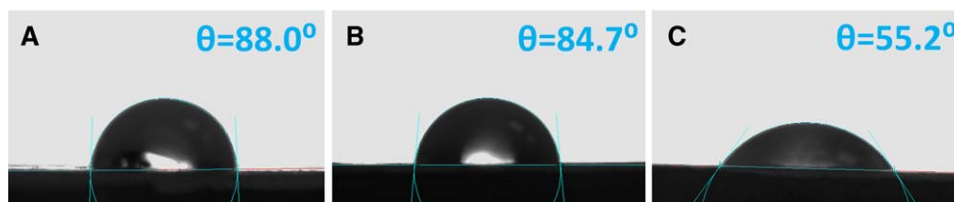
Figure 11. Water contact angles of neat PLA and PLA blend scaffold after leaching: (A) PLA, (B) PLA/NaCl (60 : 40 wt %), and (C) PLA/PEG/NaCl (50 : 10 : 40 wt %). [Color figure can be viewed in the online issue, which is available at wileyonlinelibrary.com.]

and 8 μm, and the pore density was 1.1×10^9 and 3.0×10^9. This noteworthy feature in pore morphology among these specimens can be attributed to the increased crystallization (by the incorporation of PEG), which was also found by Jenkins et al.[40]

Residual Salt Particles and PEG Content Analysis

The residual PEG and NaCl particles in the porous PLA scaffold have meaningful influence on cell/tissue cultivation. The initial and residual contents of PEG and NaCl particles in this study were determined by thermogravimetric analysis, and the results are shown in Figures 9 and 10. After leaching, as shown in Figure 9, the residual content of NaCl particles in the PLA/NaCl sample was 7 wt %, taking into consideration of the initial weight content of 40 wt %. As shown in the curve of Figure 10, the early decomposition is contributed by PEG and the residual weight is contributed by NaCl. The curve shows that the degradation of PEG occurs at the temperature from 360 to 440°C. Because PEG is soluble during the leaching process, certain amount of PEG was lost. The result shows that there is 5 wt % residual PEG after the leaching process. Moreover, the residual content of NaCl particles in the PLA/PEG/NaCl sample further decreases to 3 wt %, which was originated from the improved interconnect structure and the interface interaction between PEG and NaCl (discussed above). This implies that the foamed structure and water-soluble PEG greatly promoted the extraction of the NaCl particles. Furthermore, the residual PEG has potential to improve the PLA wettability so as to affect the property of the scaffold.

Contact Angle Measurement

For tissue engineering application, cell attachment and proliferation are closely related with the wettability of the scaffold surface. However, the cytocompatibility of the synthetic polymers including PLA, PCL, and PGA is not desirable because of their strong hydrophobicity and lack of appropriate functional groups on the surface.[41] To investigate the effect of PEG on the wetting ability of the PLA scaffolds (after leaching), the water contact angle measurements of the foams were performed, and the results are shown in Figure 11. It can be seen that neat PLA exhibits a hydrophobic surface with an average water contact angle of 88.0°. For the scaffold prepared by PLA/NaCl (60 : 40 wt %), the average water contact angle is 84.7° [Figure 11(B)], which was similar to that of PLA. Among all trials, the contact angle decreased with the increase of NaCl content, which may be due to the presence of more large pores in the scaffold with the increased NaCl content. For the scaffold prepared by PLA/PEG/NaCl (50 : 10 : 40 wt %), the contact angle declined dra-

matically to 55.2°, indicating that the incorporated amphiphilic PEG molecular chains in the matrix improve the hydrophilicity of PLA.

CONCLUSIONS

In this work, PLA blends with various PEG and NaCl weight ratios were prepared using trip-screw extruder, which improved the dispersion of NaCl in the PLA matrix. The results showed that the presence of plasticizer PEG improved the interfacial adhesion between NaCl particles and the PLA matrix. When compared with the neat PLA, the addition of PEG dramatically decreased the tensile strength of PLA/NaCl blends; however, the elongation at break of the PLA/PEG/NaCl blends increased from 6.86% to 26.34% and 11.27%. For the thermal properties, T_g and T_{cc} decreased obviously, which was probably ascribed to the fact that PEG enhanced segmental mobility of PLA molecular chains. However, the addition of PEG to PLA/NaCl blends makes the storage and loss moduli lower than those of PLA/NaCl. Neat PLA and PLA blends were foamed with CO_2 and followed by particle leaching process to investigate their foaming behavior. The morphology showed that the addition of PEG in the matrix decreased the pore size and enhanced the open-pore quantity, as well as improved the pore interconnectivity. After leaching, the bimodal porous scaffold with high interconnectivity and porosity was obtained. The porosity of PLA/PEG/NaCl (with 40 wt %) scaffold can be reached as high as 89%. Furthermore, the incorporation of PEG in the matrix further decreased the residual salt content to 3 wt % and improved the wettability of the scaffold material. Therefore, the fabricated high porosity and pore-interconnected porous scaffolds have potential to be used in tissue engineering applications.

REFERENCES

1. Shi, G. X.; Cai, Q.; Wang, C. Y.; Lu, N.; Wang, S. G.; Bei, J. Z. *Polym. Adv. Technol.* **2002**, *13*, 227.

2. Lebourg, M.; Serra, R. S.; Estelles, J. M.; Sanchez, F. H.; Ribelles, J. L. G.; Anton, J. S. *J. Mater. Sci.: Mater. Med.* **2008**, *19*, 2047.

3. Yu, H. Y.; Matthew, H. W.; Wooley, P. H.; Yang, S. Y. *J. Biomed. Mater. Res. B* **2008**, *86*, 541.

4. Hua, F. J.; Nam, J. D.; Lee, D. S. *Macromol. Rapid. Commun.* **2001**, *22*, 1053.

5. Sosnowski, S.; Wozniak, P.; Lewandowska-Szumiel, M. *Macromol. Biosci.* **2006**, *6*, 425.

6. Hou, Q. P.; Grijpma, D. W.; Feijen, J. *Biomaterials* **2003**, *24*, 1937.

7. Epple, M.; Herzberg, O. *J. Biomed. Mater. Res.* **1998**, *43*, 83.

8. Draghi, L.; Resta, S.; Pirozzolo, M. G.; Tanzi, M. C. J. S. *J. Mater. Sci.: Mater. Med.* **2005**, *16*, 1093.

9. Hong, J. K.; Madihally, S. V. *Acta Biomater.* **2010**, *6*, 4734.

10. Sultana, N.; Wang, M. J. S. *J. Mater. Sci.: Mater. Med.* **2008**, *19*, 2555.

11. Leong, K. F.; Cheah, C. M.; Chua, C. K. *Biomaterials* **2003**, *24*, 2363.

12. Riddle, K. W.; Mooney, D. J. *J. Biomater. Sci. Polym. Ed.* **2004**, *15*, 1561.

13. Lim, Y. M.; Gwon, H. J.; Shin, J.; Jeun, J. P.; Nho, Y. C. *J. Ind. Eng. Chem.* **2008**, *14*, 436.

14. Carfi Pavia, F.; La Carrubba, V.; Brucato, V. *Polym. Bull.* **2013**, *70*, 563.

15. Lu, L.; Peter, S. J.; Lyman, M. D.; Lai, H. L.; Leite, S. M.; Tamada, J. A.; Uyama, S.; Vacanti, J. P.; Langer, R.; Mikos, A. G. *Biomaterials* **2000**, *21*, 1837.

16. Gong, X. H.; Tang, C. Y.; Zhang, Y. G.; Wong, C. T.; Wu, S. P.; Liu, J. N. *J. Appl. Polym. Sci.* **2012**, *125*, 571.

17. Aydin, H. M.; El Haj, A. J.; Piskin, E.; Yang, Y. *J. Tissue Eng. Regen. Med.* **2009**, *3*, 470.

18. Kim, J. K.; Bang, S. H.; Ahmed, E. F.; Kim, H. W. *Mater. Chem. Phys.* **2014**, *143*, 1092.

19. Salerno, A.; Zeppetelli, S.; Di Maio, E.; Iannace, S.; Netti, P. A. *Biotechnol. Bioeng.* **2011**, *108*, 963.

20. Salerno, A.; Netti, P. A.; Di Maio, E.; Iannace, S. *J. Cell. Plast.* **2009**, *45*, 103.

21. Widmer, M. S.; Gupta, P. K.; Lu, L. C.; Meszlenyi, R. K.; Evans, G. R. D.; Brandt, K.; Savel, T.; Gurlek, A.; Patrick, C. W.; Mikos, A. G. *Biomaterials* **1998**, *19*, 1945.

22. Washburn, N. R.; Simon, C. G.; Tona, A.; Elgendy, H. M.; Karim, A.; Amis, E. J. *J. Biomed. Mater. Res.* **2002**, *60*, 20.

23. Ma, P. X.; Zhang, R. Y. *J. Biomed. Mater. Res.* **1999**, *46*, 60.

24. Liao, X.; Nawaby, A. V.; Naguib, H. E. *J. Appl. Polym. Sci.* **2012**, *124*, 585.

25. Rathi, S.; Chen, X. L.; Coughlin, E. B.; Hsu, S. L.; Golub, C. S.; Tzivanis, M. J. *Polymer* **2011**, *52*, 4184.

26. Turan, D.; Sirin, H.; Ozkoc, G. *J. Appl. Polym. Sci.* **2011**, *121*, 1067.

27. Jacobsen, S.; Fritz, H. G. *Polym. Eng. Sci.* **1999**, *39*, 1303.

28. Hassouna, F.; Raquez, J. M.; Addiego, F.; Dubois, P.; Toniazzo, V.; Ruch, D. *Eur. Polym. J.* **2011**, *47*, 2134.

29. Sheth, M.; Kumar, R. A.; Dave, V.; Gross, R. A.; Mccrthy, S. P. *J. Appl. Polym. Sci.* **1997**, *66*, 1495.

30. Jiang, S. B.; Liao, G. Y. *Polym. Plast. Technol. Eng.* **2012**, *51*, 1237.

31. Wang, B. Y.; Fu, S. Z.; Ni, P. Y.; Peng, J. R.; Zheng, L.; Luo, F.; Liu, H.; Qian, Z. Y. *J. Biomed. Mater. Res. A* **2012**, *100*, 441.

32. Liu, L.; Wang, Y.; Guo, S.; Wang, Z.; Wang, W. *J. Biomed. Mater. Res. B* **2012**, *100*, 956.

33. Shokrolahi, F.; Mirzadeh, H.; Yeganeh, H.; Daliri, M. *Iran. Polym. J.* **2011**, *20*, 645.

34. Zhang, W. H.; Chen, B. Y.; Zhao, H. B.; Yu, P.; Fu, D. J.; Wen, J. S.; Peng, X. F. *J. Appl. Polym. Sci.* **2013**, *130*, 3066.

35. Zeng, G. H.; Jiang, T. J.; Qu, J. P.; Liu, Y. J. *J. Appl. Polym. Sci.* **2011**, *122*, 1778.

36. Qu, J. P.; Liu, W. F.; He, H. Z. *Polym. Plast. Technol. Eng.* **2009**, *48*, 260.

37. Wei, B. H.; Qu, J. P.; Gang, X. *J. Reinforced Plast. Compos.* **2009**, *28*, 1705.

38. Jain, S.; Reddy, M. *Macromol. Mater. Eng.* **2010**, *295*, 750.

39. Park, B. S.; Song, J. C.; Park, D. H.; Yoon, K. B. *J. Appl. Polym. Sci.* **2012**, *123*, 2360.

40. Jenkins, M. J.; Harrison, K. L.; Silva, M. M. C. G.; Whitaker, M. J.; Shakesheff, K. M.; Howdle, S. M. *Eur. Polym. J.* **2006**, *42*, 3145.

41. Lin, Y.; Wang, L. L.; Zhang, P. B.; Wang, X.; Chen, X. S.; Jing, X. B.; Su, Z. H. *Acta Biomater.* **2006**, *2*, 155.